Pergamon

Journal of Structural Geology, Vol. 17, No. 3, pp. 371 to 383, 1995

0191-8141/95 $9.50+0.00

0191-8141(94)00069-7

Large volumes of anhydrous pseudotachylyte in the Woodroffe Thrust, eastern Musgrave Ranges, Australia

A. CAMACHO

Research School of Earth Sciences, The Australian National University, Canberra, A.C.T. 0200, Australia

R. H. VERNON

School of Earth Sciences, Macquarie University, Sydney, NSW 2109, Australia

and

J. D. FITZ GERALD

Research School of Earth Sciences, The Australian National University, Canberra, A.C.T. 0200, Australia

(*Received* 14 *July* 1993: *accepted in revised form* 10 *May* 1994)

Abstract—A mylonitic thrust zone, at least 1.5 km thick, forms a sharp contact between granulite and amphibolite facies gneisses in the eastern Musgrave Ranges, central Australia. The thrust dips gently to the south and is interpreted as an extension of the Woodroffe Thrust, which was formed about 550 Ma ago. Mylonites at the base of the thrust grade upwards into ultramylonites, which pass abruptly into a pseudotachylyte-bearing zone approximately 1 km thick, containing approximately 4% of pseudotachylyte veining. The orientation of the veins appears to be random. Pseudotachylytes occur only in the granulite facies rocks, and their precursors are felsic pyroxene and/or garnet granofelses. Rotated blocks of ultramylonite are present in some of the pseudotachylytes, and some pseudotachylyte veins have been plastically deformed, suggesting nearly contemporaneous semi-ductile and brittle behaviour.

The matrix of the pseudotachylyte shows spectacular examples of igneous quench microstructures, especially skeletal and dendritic crystals of plagioclase and feathery pyroxene dendrites. Also present are glass devitrification microstructures (spherulites), evidence of liquid flow, and partly melted residual grains with former glassy rims showing different optical properties from those of the surrounding isotropic material. These features confirm that the pseudotachylyte formed by melting in anhydrous conditions.

The matrix of the pseudotachylyte veins is less siliceous than the host rocks, owing to non-equilibrium melting of pyroxene, garnet and plagioclase. The igneous assemblages of the melt, notably the crystallization of pigeonite, are consistent with rapid cooling from very high-temperature (>1000°C). Melting and quenching is probably due to very local, short-lived rises in temperature accompanied by dilation.

INTRODUCTION

Large volumes of pseudotachylytes have rarely been described, apart from pseudotachylytes generated by shock metamorphism during meteoritic impact. Most workers have described thin sporadic veins associated with mylonite zones (e.g. Philpotts 1964, Sibson 1975, 1977, Grocott 1981, Passchier 1984, Hobbs *et al.* 1986, Maddock 1986, Passchier *et al.* 1990). Large veins in granulite terranes from Proterozoic shield areas have been described (e.g. Clarke 1990) but these are rarely confined to a thrust plane. This paper reports on an unusually large volume of pseudotachylyte in a major Proterozoic intracontinental mylonite zone in the eastern Musgrave Block, central Australia. It is one of the largest known thrust-related pseudotachylyte zones in the world and shows unequivocally that melt was produced during deformation.

The significance and mode of formation of pseudotachylytes have been widely discussed, often controversially (e.g. Sibson 1975, Wenk 1978, Passchier 1984, Hobbs *et al.* 1986). However, most workers have suggested that pseudotachylytes represent former melts generated by frictional heating (e.g. Philpotts 1964, Sibson 1975, Maddock 1986, Clarke 1990, Spray 1992). The microstructures of many pseudotachylytes, especially the occurrence of dendritic crystals and crystallites, imply crystallization from a melt, as in the eastern Musgrave examples. Many pseudotachylytes have the same bulk chemical compositions as their parent rocks. However, this paper will show that the eastern Musgrave pseudotachylytes have compositions different from their host rocks, as also reported from some other examples (e.g. Sibson 1975, Magloughlin 1989, Maddock 1992). This is interpreted in terms of non-equilibrium melting, with preferential dissolution of pyroxene and plagioclase. The unusually large volume of pseudotachylyte may be due to local zones of dilation acting on material heated by friction to supersolidus conditions.

REGIONAL GEOLOGICAL SETTING

The E–W-trending Musgrave Block is a Middle to Late Proterozoic mobile zone consisting of high-grade metamorphic and intrusive rocks covering an area of 120,000 km^2 in the centre of the Australian continent (Fig. 1). The eastern Musgrave Block consists of the Middle–Late Proterozoic Fregon and Mulga Park terranes, which have distinct structural and metamorphic histories (Edgoose *et al.* 1993). Both terranes are predominantly felsic gneisses, with minor horizons of mafic gneiss and granites. However, the Fregon terrane attained granulite facies conditions, whereas upper amphibolite facies gneisses of the Mulga Park terrane were unconformably overlain by the Dean Quartzite (approximately 800 Ma) and subsequently metamorphosed to upper greenschist facies. The two terranes are separated by a zone of mylonites and pseudotachylytes known as the Woodroffe Thrust (Fig. 1).

The Fregon terrane

The precursors to the granulite facies gneisses were a sequence of interlayered felsic volcanic rocks deposited some time after 1600 Ma (Gray 1978, Edgoose *et al.* 1993). Sedimentary structures are not recognized. However, thick north–south compositional layering (up to 50 m wide) is inferred to represent original lithological layering. Granulite facies metamorphism occurred at 1200 Ma ago (Gray 1978, Maboko *et al.* 1991) during two stages of deformation. F_2 folds trend N–S, are isoclinal, have a strong foliation, and overprint isoclinal F_1 folds. Granite magmatism at approximately 1150 Ma was followed by extension and emplacement of a dolerite dyke swarm at about 1050 Ma (Edgoose *et al.* 1993).

The Mulga Park terrane

Porphyritic granites and felsic gneisses form the bulk of the Mulga Park terrane. The precursors of the gneisses are unknown, but they appear to have undergone a more complex structural and metamorphic history than the Fregon terrane (Collerson *et al.* 1972, Bell 1978). The exact timing of the events is unknown, but contemporaneous upper-greenschist to lower-amphibolite facies metamorphism and thrusting occurred about 550 Ma ago in the Mulga Park terrane (Maboko *et al.* 1992). Lineations and anastomosing foliations of newly crystallized muscovite and biotite have similar orientations to structures in the Woodroffe Thrust. Therefore, these are interpreted as representing mylonitization and folding associated with thrusting.

The Woodroffe Thrust

The Woodroffe Thrust brought into contact structurally simple granulite facies rocks with more complexly folded amphibolite facies rocks (Collerson *et al.* 1972,

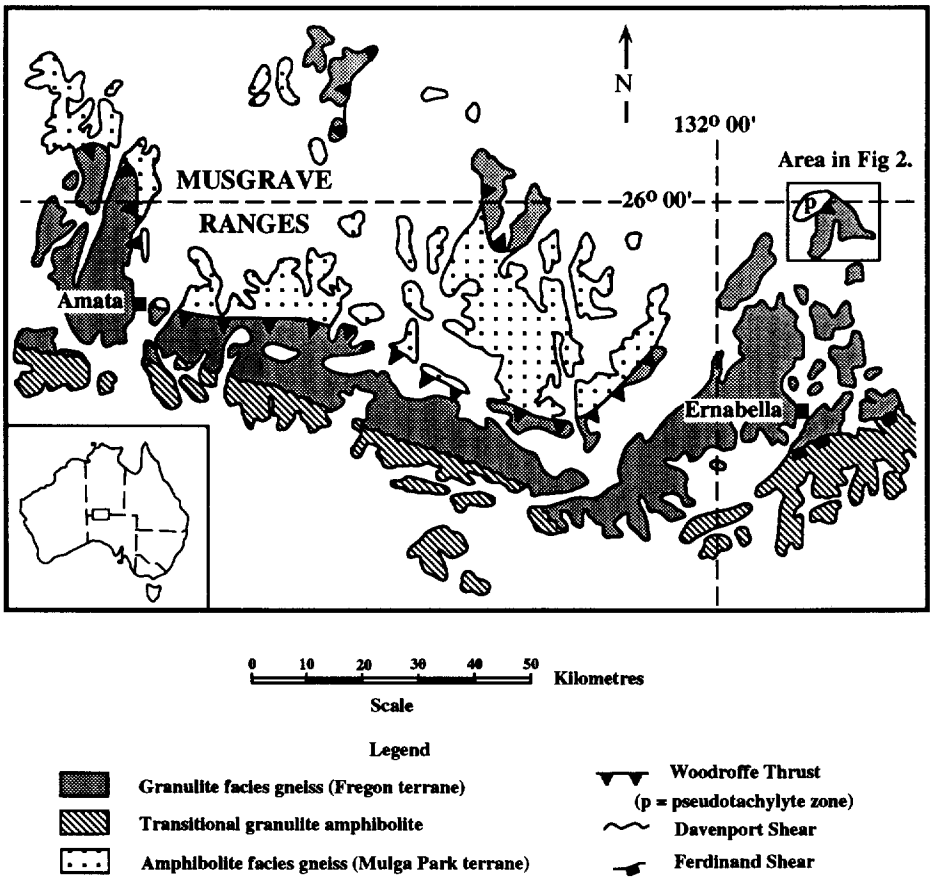

Fig. 1. Generalized geological map of the central Musgrave Block, central Australia, showing the distribution and trends of the granulite facies Fregon Terrane and amphibolite facies Mulga Park Terrane, as well as the major structural discontinuities. The Mulga Park Terrane gneisses lie below the Woodroffe Thrust.

Major 1973, Bell 1978) during the Petermann Orogeny around 550 Ma ago (Forman 1972, Maboko *et al.* 1992). The thrust forms a continuous east–west arcuate belt of mylonite and ultramylonite beneath a zone of pseudotachylyte that extends for at least 150 km and dips gently to the south (Major 1973, Bell 1978). However, the thrust may have been reactivated at several different times (Bell & Johnson 1992).

THE WOODROFFE THRUST

Mylonite–ultramylonite zone of the Woodroffe Thrust

A zone of mylonites and ultramylonites occurs at the bottom of the sequence of highly deformed rocks that make up the thrust (Fig. 2) and has an E–W foliation with a strong to extremely strong lineation that dips gently (30°) to the south. The thickness of the mylonite zone is unknown, as related anastomosing mylonitic zones occur around less deformed gneisses and granites throughout the Mulga Park terrane. Asymmetrical folds and feldspar augen, fractured and faulted feldspar grains, and the presence of granulite facies rocks overlying a lower grade terrane all suggest south over north movement. This is consistent with the published discussions on the Woodroffe Thrust by Bell (1978) and Bell & Johnson (1992).

The mylonites predominantly occur in the amphibolite facies rocks of the Mulga Park terrane. The ultramylonites are more common towards the top of the mylonite zone and grade into progressively finer grained

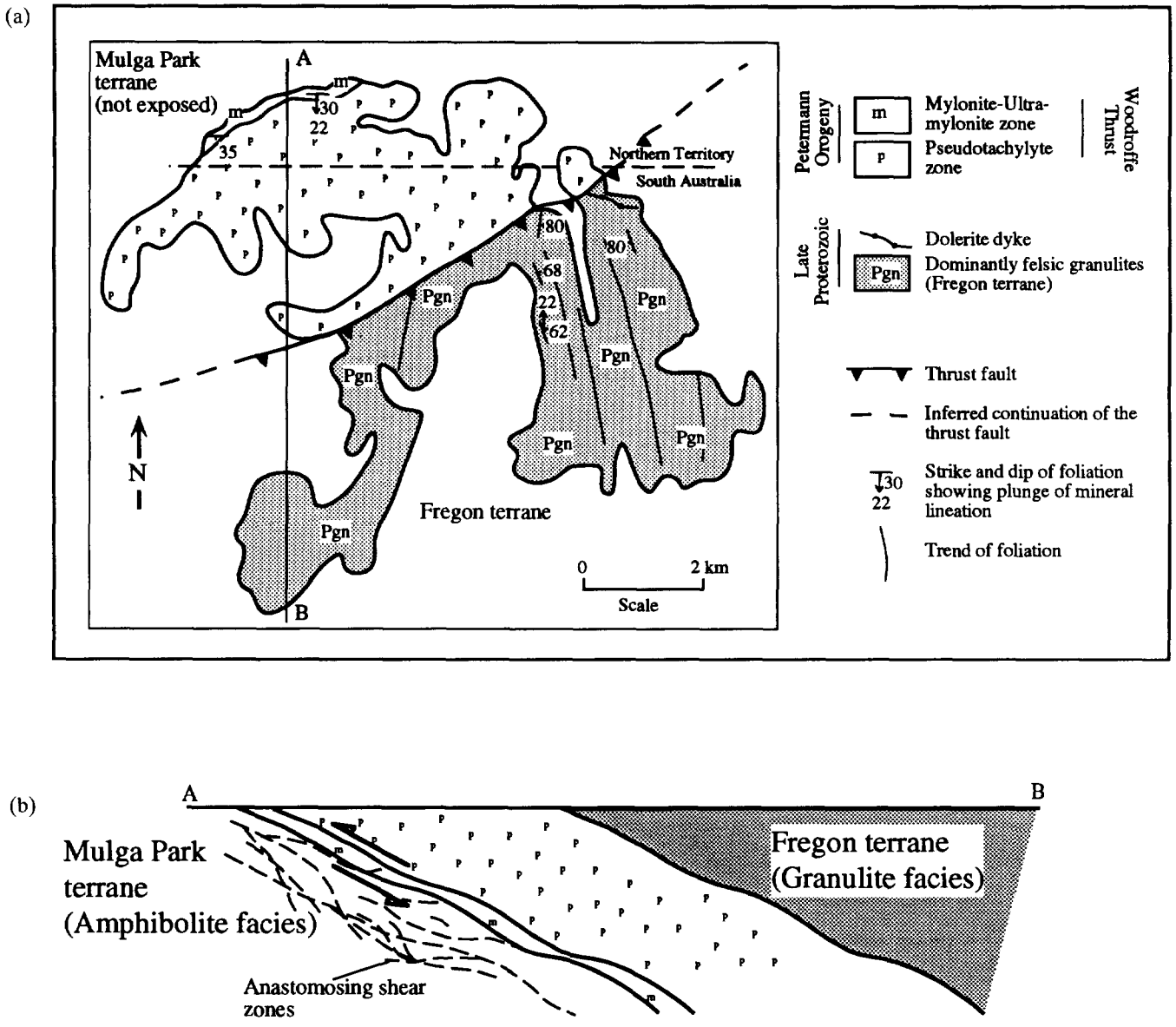

Fig. 2. (a) Geology of the Woodroffe Thrust, central Australia. The pseudotachylyte zone comprises granulite facies rocks with approximately 4% pseudotachylyte veining. (b) Schematic cross-section of the Woodroffe Thrust. The anastomosing foliations shown in dashed lines in the Mulga Park terrane represent shear zones that are related to the formation of the Woodroffe Thrust. The mylonite–ultramylonite zone is located against the amphibolite facies gneisses, whereas the granulite facies rocks do not show this ductile deformation.

mylonites and then into ultramylonites over a distance of 40 m. The ultramylonites show the same shear-sense evidence as the mylonites and form a narrow zone, up to 60 m wide, consisting of a sequence of very fine-grained, black, strongly foliated rocks. Quartz and biotite are extensively recrystallized, whereas K-feldspar, hornblende, pyroxene and garnet are not recrystallized.

Dolerite dykes in this zone are commonly boudinaged parallel to the mylonitic foliation. A mylonitic fabric is strong at the margins of the dykes and becomes progressively weaker towards the centre. Small veins of undeformed pseudotachylyte in the ultramylonite zone cut across the mylonitic foliation and commonly occur with rotated blocks of mylonite, suggesting that at least some pseudotachylyte production continued after cessation of mylonitization. In fact, the only development of pseudotachylyte in the mylonite–ultramylonite zone is confined to the dolerite dykes and transects the mylonitic fabric.

Deformed pseudotachylytes occur only in the narrow ultramylonite zone. Several criteria may be used to distinguish pseudotachylytes from ultracataclasites (e.g. Sibson 1975, Passchier 1984). Their massive and dark appearance, relative to the ultramylonites, their cross-cutting relationships and the occurrence of injection veins are the dominant identifying criteria.

The granulites also show evidence of mylonitic deformation. Normally, these occur as blocks within pseudotachylyte veins near the mylonite–ultramylonite zone. Above the thrust, the granulites are rarely mylonitic. However, where shear zones are present in the granulites, pseudotachylyte veins occur.

Pseudotachylyte zone of the Woodroffe Thrust

The ultramylonites pass abruptly into a zone rich in pseudotachylyte, approximately 1 km thick, that forms the top of the Woodroffe Thrust (Fig. 2). The dip of the pseudotachylyte zone is unknown, as no foliations or stretching lineations associated with formation of the pseudotachylyte are visible. The thickness was inferred by assuming the pseudotachylyte zone has the same attitude as the ultramylonites. The zone is confined to the granulite facies rocks and contains approximately 4% pseudotachylyte veining. The dominant precursors of the pseudotachylytes appear to be felsic granofelses. Generation surfaces are commonly difficult to recognize for the larger veins. However, pencil-thin shears commonly contain lens-shaped pockets (Sibson 1975, Magloughlin 1989) of pseudotachylyte with a geometry akin to dilational jogs in fault gouges described by Sibson (1985).

The veins are characterized by sharp contacts, commonly at an angle to layering (S_1), and by the absence of a lineation on the vein surface. They range in width from a few centimetres up to 4 m and can be traced for up to 10 m. Larger veins could not be observed, owing to the nature of the outcrop. The thinner veins are aphanitic and contain a few fragments of unmelted country rock that concentrate in the centre of the vein. Apparent chilled margins (Fig. 3a) may represent injection and crystallization of pseudotachylyte followed (not necessarily immediately) by re-opening of the same fracture by a later generation of pseudotachylyte. The presence of pseudotachylyte clasts within veins strongly support this observation. Secondary veins have propagated normal to or at an angle to the main vein. Fault and injection-vein relationships are similar to those illustrated by Sibson (1975). Paired shears, as defined by Sibson (1977) and Grocott (1981), are uncommon and where developed are partly filled by pseudotachylyte isolating rotated blocks of granulite (Fig. 3b).

The larger and more abundant pseudotachylyte veins are quasiconglomerates (Figs. 3c & d), in the sense of Sibson (1975) with large, angular to rounded clasts of unmelted rock up to 50 cm in diameter. Rock fragments are commonly rotated (Figs. 3c & d) and consist of felsic granofels, with microstructural evidence of both plastic deformation and cataclasis. In addition, some fragments consist of pseudotachylyte, which must have pre-dated the matrix pseudotachylyte. Lateral offsets associated with pseudotachylyte veining are up to 1 m, the majority showing dextral sense of displacement. These have been recognized in only a few places, owing to the lack of markers in the monotonous quartzofeldspathic sequence. The quasiconglomerate veins may represent a more advanced stage of paired shears as pseudotachylyte development progresses away from the generation surface (i.e. dilational zones).

Many episodes of melt generation must have taken place, as intersecting veins are common and earlier pseudotachylyte fragments are preserved in veins. However, these are generally difficult to distinguish, owing to the similarity in appearance between different pseudotachylyte generations and the lack of markers in the thrust zone.

The orientations of veins and shear structures containing pseudotachylyte in jogs are scattered (Fig. 5a). However, most lie at an angle of 30° or more away from the mylonitic fabric (S_m), and presumably are dilational zones that localized large amounts of melt. When the poles to the pseudotachylyte veins are contoured, a great circle can be fitted to the data (Fig. 5b). The pole to this great circle plots 50–60° from L_m and away from the plane of the mylonitic foliation (Fig. 5c). No structural significance can presently be attached to this pattern, as there is no evidence of folding after the formation of the pseudotachylyte veins.

Closely spaced (1–3 mm) near-vertical joints are present in the pseudotachylyte veins (Fig. 3d). These fractures, sub-perpendicular to the vein walls, can be traced into the surrounding mylonites and granulites, where they have a much wider spacing (50 mm). Poles to the joints plot as a great circle around the primitive (Fig. 5d) and are interpreted as representing cooling fractures akin to cooling-related columnar joints in basalts.

Above the main pseudotachylyte zone, pseudotachylyte veins (3–20 cm wide) are confined to the felsic granofelses and are generally parallel to the north–south regional layering. The veins typically are breccias, with

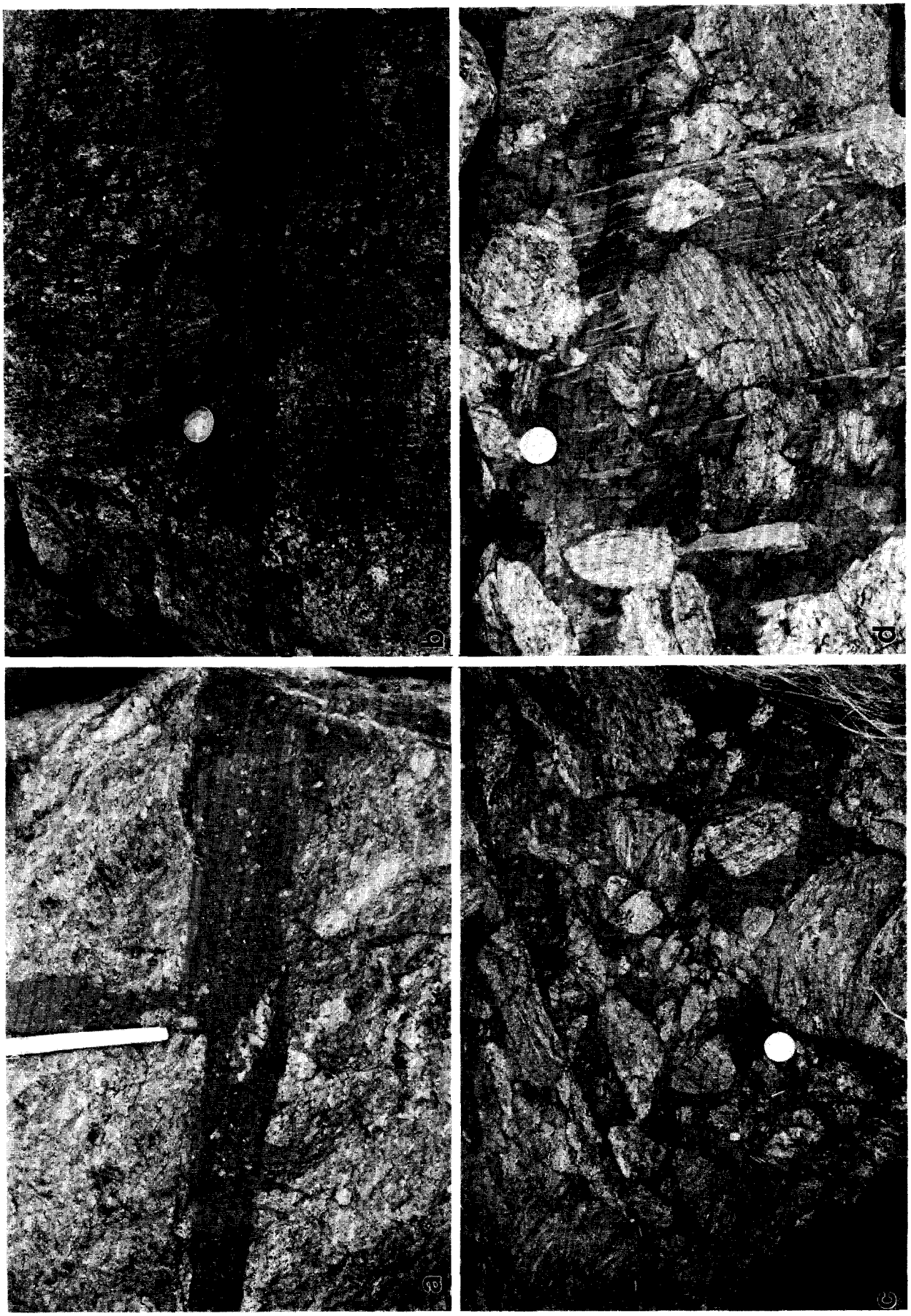

Fig. 3. (a) Apparent chilled margin probably represents episodes of vein opening. Pen length is 12 cm. (b) Paired shears. The melt is concentrated away from the generation surfaces. Note the rotated foliation in the granulite blocks within the paired shears. Coin diamcter 2.5 cm. (c) Pseudotachylyte breccia, which is a quasi-conglomerate in the sense of Sibson (1975). Coin diameter 2.5 cm. (d) Cooling fractures in pseudotachylyte breccia. The fractures are not as abundant in the granulite blocks. Coin diameter 2.5 cm.

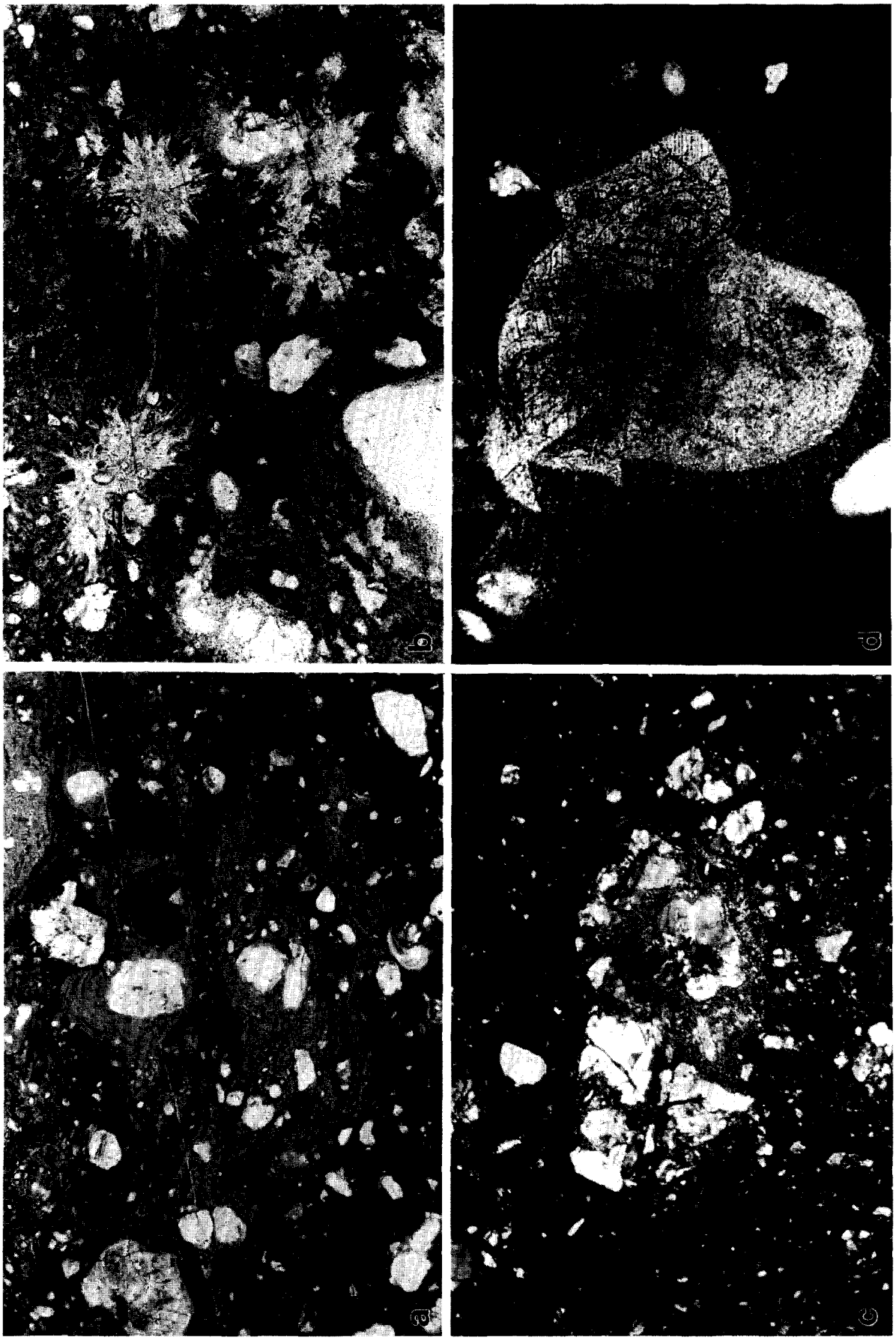

Fig. 4. (a) Clasts of plagioclase and quartz dispersed through a heterogeneous glassy matrix with flow foliation. Plane-polarized light; base of photo 4.4 mm. (b) Spherulitic aggregates formed by devitrification of glass with a flow foliation, which is deflected around clasts (bottom). Many of the clasts are rounded, owing to partial melting, and they commonly have thin rims of a different composition from that of the matrix glass. The matrix glass has a globular structure, which appears to be due mainly to similar rims on minute clasts. Plane-polarized light; base of photo 1.75 mm. (c) Clast of felsic granofels, showing fracturing of quartz and plagioclase, as well as strong subgrain structure and very fine-grained recrystallization of plagioclase. Crossed polars; base of photo 4.4 mm. (d) Kinked and fractured clast of orthopyroxene, with dendritic pyroxene outgrowths. Planc-polarized light; base of photo 0.70 mm.

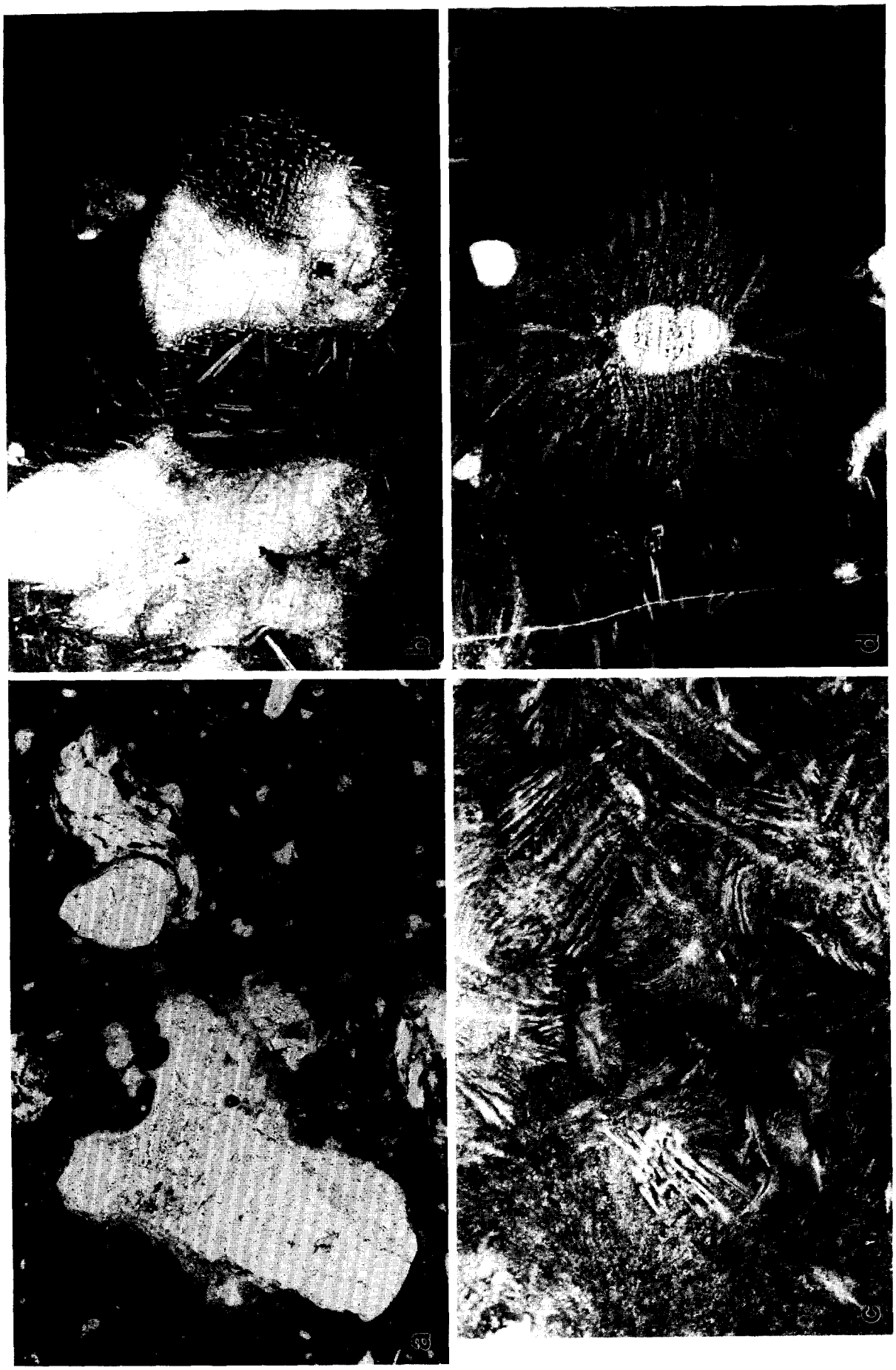

Fig. 6. (a) Rock clast with deformed, fractured but unmelted quartz and largely melted feldspar (left), with smaller clast of quartz with melted feldspar flowing around it (right). Plane-polarized light; base of photo 0.70 mm. (b) Skeletal plagioclase fringes on rounded and deeply corroded clasts of plagioclase. Skeletal plagioclase crystals and acicular pyroxene microlites are present in the glassy matrix. Plane-polarized light; base of photo 0.70 mm. (c) Feathery dendrites of pyroxene and local skeletal plagioclase. Plane-polarized light; base of photo 0.70 mm. (d) Feathery outgrowth of pyroxene developed on, and in optical continuity with, a rounded clast of orthopyroxene. Plane-polarized light; base of photo 0.70 mm.

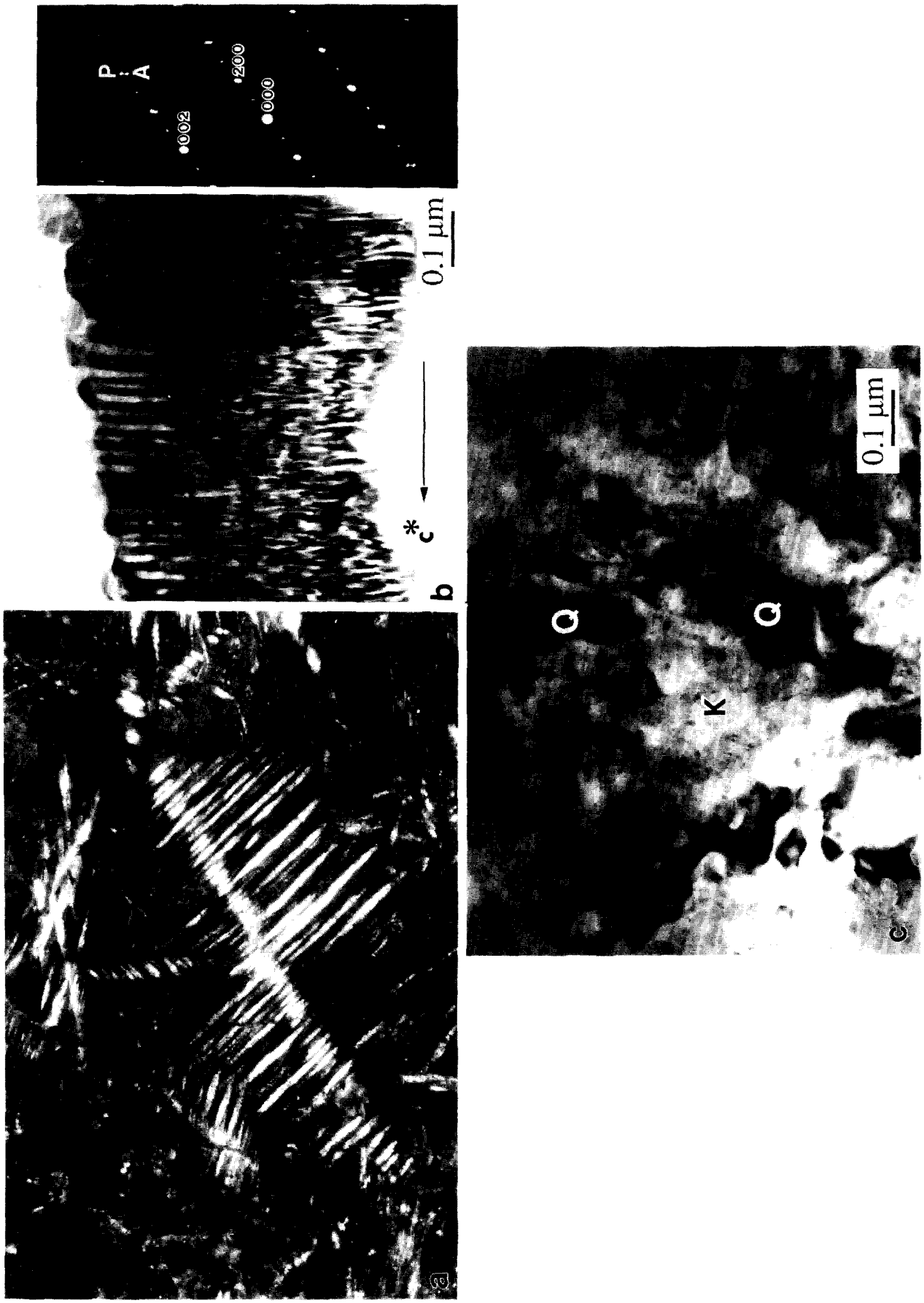

Fig. 7. (a) Skeletal dendrites of clinopyroxene imaged in an ultra-thin section using crossed-polarized light. The skeletal structure arises from alignment of [001] needles of pyroxene. Base of photo 0.35 mm. (b) (001) Exsolution lamellae in the pyroxene needles. The bright field TEM image is from one needle of pyroxene viewed approximately along its [100] axis. The trace of the [001] needle axis is parallel to c^* in the image. Narrow lamellae run from top to bottom of this image. The [010] electron diffraction pattern on the right is from a different needle and is included to show intergrown pigeonitic (indicated by P on the pattern) and augitic (A) pyroxene. The reflections from both pyroxenes are consistent with the expected space groups ($P2_1/c$ for pigeonite and $C2/c$ for augite), though the orientation between the two lattices is close to, but not exactly, that expected for (001) lamellae. (c) Fine grained mesostasis encountered between larger grains of pyroxene and plagioclase, as viewed in bright field TEM. Some grains of quartz (Q) are dark because they are oriented for strong diffraction. The intervening bright grains are a mixture of other, unoriented quartz and K-feldspar (K). Note also the tiny (*ca.* 0.01 μm) dark specks of magnetite throughout this area.

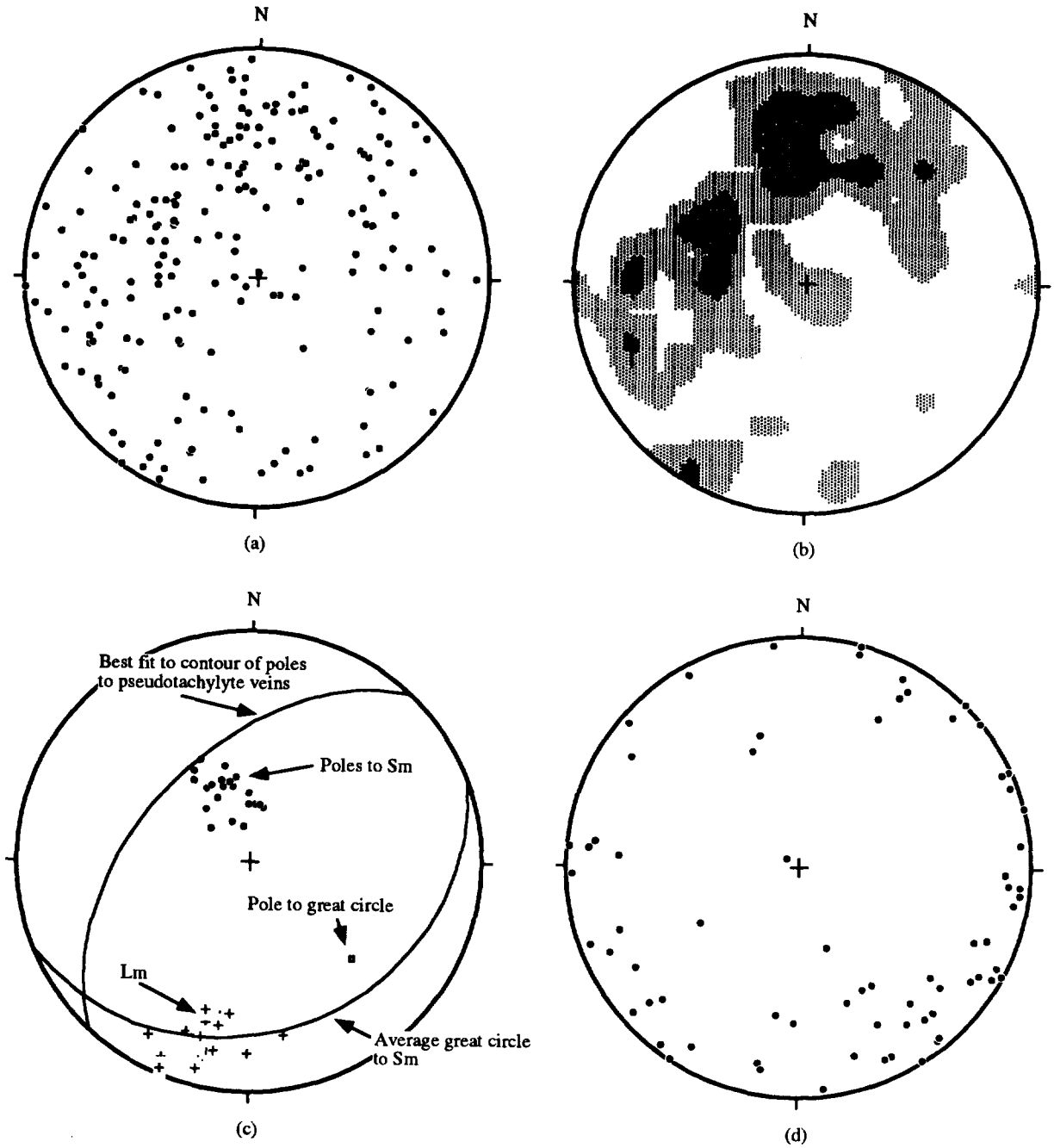

Fig. 5. (a) Stereographic projection of poles to veins and generation surfaces containing melt (n = 205). Schmidt equal-area projection. (b) Contoured diagram of poles to veins and generation surfaces containing melt. Contours at 1, 2, 3, 4 and 5 times uniform. Schmidt equal-area projection. (c) Summary of structural data for the Woodroffe Thrust. (d) Stereographic projection of the poles to joints (n = 73). Schmidt equal-area projection.

clasts of felsic granofels surrounded by black pseudotachylyte.

Microstructures, mineralogy and petrology of the pseudotachylytes

The pseudotachylytes consist of partly melted clasts dispersed through heterogeneous matrix (Figs. 4a, 6a & b), much of which is optically isotropic. In many places, the matrix has a globular structure, which appears to be due mainly to optically isotropic rims on small, rounded clasts, the rims having a different composition from that of the adjacent matrix (Figs. 4a & 6a). Colour differences suggest that some parts of the matrix have different compositions from others (Fig. 4a). Some lenticular, optically isotropic patches have a well-developed flow foliation (Fig. 4a). Locally, very finely recrystallized aggregates of quartz and feldspar are elongate in the foliation, and may be contorted, in conformity with folds in the foliation.

Spherulitic aggregates are very common (Fig. 4b). They probably formed by devitrification of glass, rather than by crystallization from melt, arguing by analogy with spherulites in glassy volcanic rocks. This interpre-

Table 1. XRF (samples 1 and 2) and electron microprobe analyses (samples 3 and 4) in wt. % of felsic granulite and pseudotachylyte veins from the Woodroffe Thrust

Sample	1	2	3	4
SiO_2	73.91	72.20	63.03	62.34
TiO_2	0.31	0.34	0.77	0.66
Al_2O_3	13.48	12.36	18.05	18.00
FeO total	1.44	3.19	5.11	5.39
MnO	0.06	0.07	0.24	0.22
MgO	0.65	1.41	2.05	2.12
CaO	1.54	2.31	2.96	3.00
Na_2O	3.21	2.57	4.77	5.00
K_2O	4.87	4.47	2.92	2.66
Total	99.47	98.92	99.89	99.38

1—Average felsic gneiss (4 samples).
2—Pseudotachylyte vein.
3—Representative analysis of pseudotachylyte matrix free of clasts. This fraction contains crystals that appear to have crystallized from a melt. Area measured 50 μm^2.
4—As for analysis 3. Area measured 12.5 μm^2.

tation is supported by the fact that flow foliae are truncated by the spherulitic aggregates, whereas they are deflected around clasts (Figs. 4a & b).

The clasts vary in shape from angular to rounded, and in size from relatively large to submicroscopic quartz–feldspar fragments (Figs. 4d and 6a). Feldspar and quartz are the dominant minerals in clasts, whereas ferromagnesian clasts are rare. Consequently, the clast fraction of the pseudotachylyte is quite different from that in the host rock assemblage. Feldspar clasts commonly show intense fracturing, subgrain structure and recrystallization to very fine-grained aggregates (Fig. 4c). Pyroxene clasts commonly show undulatory extinction, kinking and fracturing (Fig. 4d), and many have been altered to very fine-grained opaque material. Most clasts of feldspar and pyroxene are rounded and embayed to varying degrees, owing to dissolution in the melt (Fig. 6d). Pyroxene and quartz clasts commonly have high concentrations of opaque inclusions.

The inferred melt fraction contains skeletal to dendritic crystallites and microlites (Figs. 6d–7b) which, from analogy with volcanic rocks and from experimental crystallization of plagioclase (Lofgren 1980), indicate crystallization from a melt rather than glass. In addition, the optically isotropic material from the Musgraves is not truly amorphous, but is an aggregate of submicron-sized crystals of clinopyroxene and plagioclase, which is consistent with other work on pseudotachylyte (e.g. Wenk & Weiss 1982).

Raster-scan microprobe analyses of several regions that are optically isotropic and clast-free give compositions that are more mafic than the whole-rock analysis (Table 1). The intention behind the raster-scan measurements was to minimize alkali loss (Spray 1993). Assuming such analyses to be representative of the matrix component, and hence the original melt fraction, of the pseudotachylyte (Bossière 1991, Maddock 1992), the implication is that mafic to intermediate melts can be produced by the partial melting of felsic rock (e.g. Sibson 1975, Magloughlin 1989, Maddock 1992). In addition, Webb (1983) showed that the pseudotachylytes from the Musgrave Block have the same $^{87}Rb/^{86}Sr$ initial ratios as their host, suggesting that the melting occurred in a closed system.

Plagioclase. Plagioclase is relatively homogeneous (An_{30-40}) and occurs as acicular, arrow-head and hopper crystals (Figs. 6b–d), many of which form outgrowths on plagioclase clasts.

Clinopyroxene. Clinopyroxene occurs as abundant feathery and skeletal dendrites (Figs. 6c–7a). At the submicron scale, the laths are exsolved, and transmission electron diffraction patterns show them to be intergrown pigeonite and augite (Fig. 7b). The overall composition is subcalcic, the Mg number and CaO content ranging from 45–60 and 4–10 wt.%, respectively (analyses by EDS in electron microprobe and analytical TEM). Consequently, these clinopyroxenes are dominantly pigeonitic and reinforce the microstructural evidence of crystallization from a high-temperature melt.

Mesostasis. Between the submicron-sized plagioclase and clinopyroxene crystals, even finer-grained intergrowths of quartz and K-feldspar are visible in the TEM (Fig. 7c). These are interpreted as the last fraction of melt to crystallize and are akin to the mesostasis found in chilled dolerites.

Magnetite. Magnetite occurs mainly in the glassy and newly crystallized material with grain size ranging from 20 μm–5 nm. However, it tends to be concentrated in fracture planes in quartz clasts. The presence of this newly crystallized mineral makes the pseudotachylyte veins more magnetic than the host. The palaeomagnetic implications are currently being investigated.

Water content. No hydrous minerals are present in material examined using TEM. In addition, analytical totals (Table 1) indicate $< 1\%$ H_2O in the pseudotachylyte (some of which could be due to limonitic weathering) and for granitic compositions this corresponds to a low water activity of 0.13 in the melt. No amygdales occur in the Musgrave pseudotachylytes, in comparison to amygdale-bearing examples that Maddock *et al.* (1987) concluded had formed near the surface with significant water activity. We conclude that the Musgrave pseudotachylytes formed from relatively anhydrous melts.

DISCUSSION

Cyclical development of mylonite and pseudotachylyte has previously been recognized (e.g. Sibson 1980, Passchier 1984, Passchier *et al.* 1990). This feature has been used to suggest that pseudotachylytes formed either in (i) the ductile regime (Hobbs *et al.* 1986) or (ii) the brittle–ductile transition (Passchier 1984, Passchier *et al.* 1990). In the Woodroffe Thrust, the cyclical development of the mylonites and pseudotachylytes

appears to be a feature of pseudotachylytes close to the mylonite–ultramylonite zone. Elsewhere in the pseudotachylyte zone, the pseudotachylytes are not plastically deformed, and we interpret this as representing lithological control over the style of deformation. The possibility that the large volumes of pseudotachylyte in the granulite facies gneisses formed late in the history of the Woodroffe Thrust is rejected because large volumes of undeformed pseudotachylyte should also be present throughout the mylonite–ultramylonite zone and this is not observed.

The presence of large volumes of melt and pseudotachylyte clasts in the thicker veins suggests a long history of melt-forming events. The application of Mohr diagrams (e.g. Hobbs *et al.* 1976) can be used to simplistically envisage the cyclical development of pseudotachylyte and mylonite. Consider a situation where anhydrous granulites are thrust onto a hydrous amphibolite facies terrane, both being subjected to similar regional stresses. Granulite and amphibolite facies rock-types have different fracture and plastic behaviour related to the different content of hydrous minerals. As the differential stress (σ_1–σ_3) increases, hydrated rocks tend to deform plastically, whereas the anhydrous material responds elastically. As the radius of the Mohr circle increases due to the increase in σ_1, the failure envelope of the granulites is reached first and shear fracture occurs in this rock type. Shear failure is expected to be accompanied by transient stress relief (i.e. a decrease in σ_1). However, heat generation due to friction causes partial melting of the granulites during shear failure, creating a near lithostatic pressured melt which reduces the effective stress. If the differential stress falls below 4T (T = tensile strength of the granulites) during the failure process, the Mohr circle may intersect the failure envelope in the tensile region resulting in hydraulic extension fracturing. These extension fractures then drain the melt from the generation surface adjacent to the failure surface. The melt then quenches, so that the fluid pressure is effectively removed, and the effective stresses again increase. Note that melt migration from generation surfaces can also occur at higher differential stress levels if dilational jogs open during shear failure. We contend that repetitions of this cycle for the Musgrave examples can explain (i) the cyclical development of pseudotachylytes and mylonites, (ii) why most generation surfaces do not preserve melt other than in dilational jogs, injection veins and paired shears, (iii) the lack of plastic deformation in the granulites, and (iv) why dolerite dykes in the mylonite zone contain pseudotachylyte veins.

The foregoing observations suggest that the pseudotachylytes in the Woodroffe Thrust formed under conditions of low water activity in the melt (*ca.* 0.1) by non-equilibrium melting, as the silica content in the melt is lower than the host gneisses. Rapid crystallization followed probably near equilibrium, as inferred from the crystallization sequence. The mylonites and ultramylonites have mineral assemblages indicative of the upper greenschist facies, whereas the pseudotachylytes have igneous assemblages indicating high-temperature crystallization, including crystallization of pigeonite. Pseudotachylytes need to be at approximately 4–5 km depth (approx 1.5 kbar) to produce melting at 1100°C (Sibson 1975). In the Musgrave examples at 1.5 kbar, the temperature must have increased from 400°C (the likely temperature of the country rock) to greater than 900°C (minimum stability temperature for pigeonite with an Mg number between 45–60, Lindsley 1983), with melting initiated as a result of very local, short-lived rises in temperature (frictional heating), while the surrounding rocks remained much cooler. Furthermore, the relatively small volumes of melt produced at each shear increment (owing to the low water activity) must have been followed by dilation to restore the shear surface and allow more frictional displacement. In effect, dilational zones serve the dual purpose of promoting further melting adjacent to 'generation surfaces' and being receptacles for the melt generated.

Pseudotachylyte veins, including those in the eastern Musgrave Ranges, characteristically contain few ferromagnesian mineral fragments (e.g. Sibson 1975, Maddock 1986, Macaudiere *et al.* 1985). The pseudotachylyte matrix (Table 1) is high in Ca and Fe, suggesting preferential breakdown of most of the mafic constituents in the granulite facies rocks, which have low abundances of mafic minerals. The rarity of orthopyroxene clasts and the lack of garnet clasts is consistent with this observation. Maddock (1986) showed that partial melting from shear heating occurs to a greater degree in and around sites occupied by hydrous mafic minerals. However, the pseudotachylyte precursors in the Musgrave Block characteristically lack hydrous phases. Moreover, Sibson (1975) has shown that the presence of water would limit temperature rises to small amounts (probably around 100°C), thereby inhibiting the formation of pseudotachylytes. Thus, the large volumes of pseudotachylyte in the eastern Musgrave Ranges appear to have developed in anhydrous rocks.

Bulk chemical analyses of the pseudotachylyte are very similar to those of the host (Table 1), which is the usual situation observed world-wide (e.g. Philpotts 1964, Sibson 1975, Clarke 1990), although some studies have found differences (e.g. Teschmer *et al.* 1992). Similarity of composition is not surprising, because bulk samples of pseudotachylyte contain clasts, and the rocks generally show no evidence that any melt migrated out of the rock. However, in pseudotachylytes of the Outer Hebrides Thrust Zone, Sibson (1975) subtracted the compositions of porphyroclasts from the bulk pseudotachylyte analysis and concluded that the matrix (melt fraction) had a basaltic andesite composition. The matrices of the Woodroffe Thrust pseudotachylytes are also less siliceous than their host (Table 1). Preferential melting of the mafic fraction in the host rock (e.g. Magloughlin 1989, Maddock 1992, Spray 1993) can explain the differences in composition between the host and the pseudotachylyte matrix (inferred melt fraction).

Evidently, the quartz in the Musgrave examples was not as strongly plastically deformed or fractured as the

feldspar and pyroxene under the exceptionally dry conditions of deformation, and so it did not dissolve as readily. In fact, quartz had never been reported as a newly crystallizing material in pseudotachylyte, to the best of our knowledge, so that this may be a general phenomenon. On the other hand, plagioclase and pyroxene were very strongly plastically deformed and fractured and the pyroxene also commonly has been altered to opaque material, which could have assisted melting. Sibson (1975) reported that clasts of quartz have sharp edges, whereas clasts of feldspar have embayed and fuzzy edges, which he interpreted as being due to preferential melting of feldspar. All these observations are consistent with our analyses of matrix composition (carefully conducted to avoid clasts) being significantly different from the host rock composition.

CONCLUSIONS

During thrusting in the Musgrave Ranges, large volumes of pseudotachylyte preferentially formed in anhydrous felsic granulites, but in vastly smaller volumes in underlying amphibolite facies rocks. These pseudotachylytes have a high proportion of unmelted quartz and feldspar clasts. The matrix shows excellent examples of microstructures formed by rapid crystallization from high-temperature melts. Pseudotachylyte veins have similar bulk compositions to those of the surrounding granulites, which is due to the abundance of clasts. However, the matrix fractions of the pseudotachylytes represent anhydrous melts of intermediate composition. We suggest these can be produced from more felsic hosts by preferential melting of ferromagnesian minerals and plagioclase at low water activities.

Skeletal pigeonite and plagioclase crystals indicate quench crystallization of a melt at relatively high temperatures, perhaps as much as 1200°C. This temperature is much higher than the inferred 400°C of the surrounding rocks and probably resulted from numerous, local, short-lived frictional heating events.

Mechanical behaviour was very much dependent on rock composition. Mylonitic deformation in amphibolite facies rocks is inferred to have been contemporaneous with pseudotachylyte development in the adjacent granulite facies terrane, both occurring at greenschist facies conditions. Microstructures and mesostructures in the Musgrave samples indicate multiple pseudotachylyte injection events that may reflect repeated stress cycles. In contrast to an interpretation that other pseudotachylytes are formed where country rocks are at some critical level in Earth's crust so as to straddle their brittle-ductile transition, we argue for cyclic pseudotachylyte development associated with dilation resulting from hydraulic fracturing in the presence of a melt.

Acknowledgements—This paper is published with the permission of the Director, Northern Territory Geological Survey. We are particularly grateful for the advice and assistance of those who critically reviewed this paper and to Stephen Cox for helpful discussions regarding pseudotachylytes in general. In addition, we appreciate the constructive comments of J. G. Spray, R. J. Norris and an anonymous reviewer.

REFERENCES

Bell, T. H. 1978. Progressive deformation and reorientation of fold axes in a ductile mylonite zone: The Woodroffe Thrust. *Tectonophysics* **44**, 285–320.

Bell, T. H. & Johnson, S. E. 1992. Shear sense: a new approach that resolves conflicts between criteria in metamorphic rocks. *J. Metamorphic Geol.* **10**, 99–124.

Bossière, G. 1991. Petrology of pseudotachylytes from the Alpine Fault of New Zealand. *Tectonophysics* **196**, 173–193.

Clarke, G. L. 1990. Pyroxene microlites and contact metamorphism in pseudotachylyte veinlets from MacRobertson Land, east Antarctica. *Aust. J. Earth Sci.* **37**, 1–8.

Collerson, K. D., Oliver, R. L. & Rutland, R. W. R. 1972. An example of structural and metamorphic relationships in the Musgrave Orogenic Belt, central Australia. *J. geol. Soc. Aust.* **18**, 379–393.

Edgoose, C., Camacho, A., Wakelin-King, G. W. & Simons, B. 1993. Kulgera, 1:250 000 Geological Series. Northern Territory Geological Survey Explanatory Notes, SG53-5.

Forman, D. J. 1972. Petermann Ranges, 1:250 000 Geological Series. Bureau of Mineral Resources, Australia, Explanatory Notes, SG52-7.

Gray, C. M. 1978. Geochronology of granulite facies gneisses in the western Musgrave Block, central Australia. *J. geol. Soc. Aust.* **25**, 403–414.

Grocott, J. 1981. Fracture geometry of pseudotachylyte generation zones: a study of shear fractures formed during seismic events. *J. Struct. Geol.* **3**, 169–178.

Hobbs, B. E., Means, W. D. & Williams, P. F. 1976. *An Outline of Structural Geology*. Wiley, New York.

Hobbs, B. E., Ord, A. & Teyssier, C. 1986. Earthquakes in the ductile regime? *Pure & Appl. Geophys.* **124**, 309–336.

Lindsley, D. H. 1983. Pyroxene thermometry. *Am. Miner.* **68**, 477–493.

Lofgren, G. 1980. Experimental studies on the dynamic crystallization of silicate melts. In: *Physics of Magmatic Processes* (edited by Hargraves, R. B.). Princeton University Press, Princeton, pp. 487–551.

Maboko, M. A. H., McDougall, I., Zeitler, P. K. & Williams, I. S. 1992. Geochronological evidence for ~530–550 Ma juxtaposition of two Proterozoic metamorphic terranes in the Musgrave Ranges, central Australia. *Aust. J. Earth Sci.* **39**, 457–471.

Maboko, M. A. H., Williams, I. S. & Compston, W. 1991. Zircon U–Pb chronometry of the pressure and temperature history of granulites in the Musgrave Ranges, central Australia. *J. Geol.* **99**, 675–697.

Macaudiere, J., Brown, W. L. & Ohnenstetter, D. 1985. Microcrystalline textures resulting from rapid crystallization in a pseudotachylite melt in a meta-anorthosite. *Contr. Miner. Petrol.* **89**, 39–51.

Maddock, R. H. 1986. Partial melting of lithic porphyroclasts in fault-generated pseudotachylytes. *Neues Jb. Miner. Abh.* **155**, 1–14.

Maddock, R. H. 1992. Effects of lithology, cataclasis and melting on the composition of fault-generated pseudotachylytes in Lewisian gneiss, Scotland. *Tectonophysics* **204**, 261–278.

Maddock, R. H., Grocott, J. and Van Nes, M. 1987. Vesicles, amygdales and similar structures in fault-generated pseudotachylytes. *Lithos* **20**, 419–432.

Magloughlin, J. F. 1989. The nature and significance of pseudotachylite from the Nason terrane, North Cascade Mountains, Washington. *J. Struct. Geol.* **11**, 907–917.

Major, R. B. 1973. Woodroffe, South Australia, 1:250 000 Geological Series. South Australian Department of Mines and Energy, Explanatory Notes, SG52-12.

McKenzie, D. and Brune, J. N. 1972. Melting on fault planes during large earthquakes. *Geophys. J. R. Astr. Soc.* **29**, 65–78.

Passchier, C. W. 1984. The generation of ductile and brittle shear bands in a low-angle mylonite zone. *J. Struct. Geol.* **6**, 273–281.

Passchier, C. W., Hoek, J. D., Bekendam, R. F. & De Boorder, H. 1990. Ductile reactivation of Proterozoic brittle fault rocks; an example from the Vestfold Hills, East Antarctica. *Precambrian Res.* **47**, 3–16.

Philpotts, A. R. 1964. Origin of pseudotachylites. *Am. J. Sci.* **262**, 1008–1035.

Sibson, R. H. 1975. Generation of pseudotachylite by ancient seismic faulting. *Geophys. J. R. Astr. Soc.* **43**, 775–794.

Sibson, R. H. 1977. Fault rocks and fault mechanisms. *J. geol. Soc. Lond.* **133**, 191–213.

Sibson, R. H. 1980. Transient discontinuities in ductile shear zones. *J. Struct. Geol.* **2**, 165–171.

Sibson, R. H. 1985. Stopping of earthquake ruptures at dilational fault jogs. *Nature* **316**, 248–251.

Spray, J. G. 1992. A physical basis for the frictional melting of some rock-forming minerals. *Tectonophysics* **204**, 205–221.

Spray, J. G. 1993. Viscosity determinations of some frictionally generated silicate melts: implications for fault zone rheology at high strain rates. *J. geophys. Res.* **98**, 8053–8068.

Teschmer, K. S., Ahrendt, H. & Weber, K. 1992. The development of pseudotachylyte in the Ivrea–Verbano Zone of the Italian Alps. *Tectonophysics* **204**, 307–322.

Wenk, H. R. 1978. Are pseudotachylites products of fracture or fusion? *Geology* **6**, 507–511.

Wenk, H. R. & Weiss, L. E. 1982. Al-rich calcic pyroxene in pseudotachylite: an indicator of high pressure and high temperature? *Tectonophysics* **84**, 329–341.